HOKKAIDO UNIVERSITY

Title	Phytotoxicity of multi-walled carbon nanotubes on red spinach (Amaranthus tricolor L) and the role of ascorbic acid as an antioxidant
Author(s)	Begum, Parvin; Fugetsu, Bunshi
Citation	Journal of Hazardous Materials, 243, 212-222 https://doi.org/10.1016/j.jhazmat.2012.10.025
Issue Date	2012-12
Doc URL	https://hdl.handle.net/2115/52048
Type	journal article
File Information	JHM243_212-222.pdf



Hokkaido University Collection of Scholarly and Academic Papers : HUSCAP

Phytotoxicity of multi-walled carbon nanotubes on red spinach (*Amaranthus tricolor* L) and the role of ascorbic acid as an antioxidant

Parvin Begum and Bunshi Fugetsu*

Laboratory of Environmental Medical Chemistry, Graduate School of Environmental Science, Hokkaido University, Sapporo 060-0810, Japan

* *Corresponding author*: Fax: 81 11 7062272

E-mail address: hu@ees.hokudai.ac.jp (B. Fugetsu).

Abstract

Carbon nanotubes (CNTs) are a novel nanomaterial with wide potential applications; however the adverse effects of CNTs following environmental exposure have recently received significant attention. Herein, we explore the systemic toxicity and potential influence of 0–1000 mg L^{-1} the multi-walled CNTs on red spinach. CNTs exposed plants exhibited growth inhibition and cell death after 15 days of hydroponic culture. CNTs had adverse effects on root and leaf morphology, as observed by scanning electron microscopy (SEM) and transmission electron microscopy (TEM). Raman spectroscopy detected CNTs in leaves. Biomarkers of nanoparticle toxicity, reactive oxygen species (ROS), and cell damage in the red spinach were greatly increased 15 days post-exposure to CNTs. These effects were reversed when CNTs were supplemented with ascorbic acid (AsA), suggesting a role of ROS in the CNT-induced toxicity and that the primary mechanism of CNTs' toxicity is oxidative stress.

Keywords: Multi-walled carbon nanotubes; Red spinach (*Amaranthus tricolor* L); Reactive oxygen species; Phytotoxicity; Ascorbic acid

1. Introduction

Carbon nanotubes (CNTs) are increasingly used as key-materials for applications at industrial quantities to meet numbers of nano-technological demands [1, 2]. Concerning the possible human exposure, it is important to consider the uptake of CNTs in media and organisms that are routinely consumed by humans (e.g., plant, vegetables, and fish). While the tremendous positive impacts of nanotechnology are widely publicized, studies of potential threats or risks to human health and the environment are just beginning to emerge [3]. After penetrating the body through the food web, CNTs may be harmful to humans [4]. The unique nanometer-scale structure of CNTs is based on a graphene cylinder that is typically a few nanometers in diameter and can range in length from a few micrometers to millimeters [5]. Ingestion of the CNTs can result in adverse biological effects [6]. Parallel to CNTs, the so-called zero-dimensional nano-particles, such as carbon blacks, silica, titanium oxide, alumina, iron oxide, and zirconium oxide had been also investigated [7 – 9]; they were found to be toxic to plants but with relatively lower toxicity [10 - 13].

Plants and plant cells showed high tendencies to accumulate CNTs [14, 15], making plants an important link in the pathway by which CNTs enter the food chain and

biological cycles [16]. Torney and co-wokers [17] demonstrated that CNTs can assist the delivery of biological molecules into plant cells. Abundant studies [18 - 21] have demonstrated that CNTs can cause pronounced toxicity to plants. Tan et al. [22] and Canas et al. [23] described seed germination and growth inhibition induced by CNTs in selected plants and plant cells. The higher sensitivity to CNTs may be a universal biological phenomenon, as it has also been observed in human [24], animal [25], and bacteria [26] systems. The threshold at which symptoms of toxicity become established differs widely among plant species, and the impact of nano-particles on different plant species can vary greatly, depending on the plant growth stage, the method and the duration of exposure, as well as on the nano-particle size, concentration, chemical composition, surface structure, solubility, shape, and aggregation [27]. The varying experimental conditions used in different studies make it difficult to rigidly classify plants into tolerance groups. Some broad generalizations are possible, but there is a vital need to examine the possible toxicity of CNTs to diverse crop species.

Reactive oxygen species (ROS) generation and oxidative stress have been suggested as primary mechanisms by which CNTs alter plant cell growth [20, 28] . ROS generation and oxidative stress can lead to cell membrane, mitochondria, and DNA

damage [29], which could ultimately impact the whole organism in terms of development, reproduction, and viability. Response to oxidative stress involves the induction of antioxidant molecules and detoxification enzymes [30].

We conducted a preliminary screening to determine CNTs' phytotoxicity toward seven plant species (chili, cucumber, lady's finger, lettuce, red spinach, rice, and soybean) [31]. The vegetative plant red spinach was selected for further study, since its roots and leaves both displayed toxic symptoms and its small seed size results in a relatively large surface area to volume ratio, which is conductive to higher sensitivity to toxicants [32]. The present study investigated the adverse impact of CNTs on red spinach and discovered these effects to be mediated by oxidative stress, underscoring the importance of nanomaterial presentation to the phytotoxic response. We also showed, for the first time in an *in vivo* study, the alleviation of CNTs toxicity by treatment with the antioxidant ascorbic acid (AsA).

2. Experimental

2.1. Nanomaterials, chemicals, and seeds

The multi-walled CNTs were purchased from CNano Technology Ltd., China. The as-received, raw CNTs were powders with a loose agglomerate size of 0.1–0.3 mm, outer mean diameter of ~11 nm, inner mean diameter of ~4 nm, and length of >1 μm. The CNTs powders were first wetted overnight with deionized water at about 40 °C. The water-wetted CNTs powders were then milled into smaller sizes with a continuously operating bead-mill system, without adding any kind of dispersants (surfactants). The water-wetted milled CNTs were used throughout this study. For AFM (Atomic force microscopy), an Agilent Series 5500 AFM instrument was used. The samples were prepared by casting a diluted aqueous CNTs suspension on the surfaces of mica. The images were obtained using the tapping mode at a scanning rate of 1 Hz. The morphology of CNTs, root and leaf were investigated using S-4000 scanning electron microscope (SEM) and a Hitachi H-800 Transmission electron microscope (TEM). For analyzing the samples using SEM, a drop of the CNTs suspension were deposited on the aluminium stub, dried and sputter-coated before the analysis. For the roots and leaves, the samples were fixed in 2.5% glutaraldehyde (GA) and 2% paraformaldehyde (PA) in 0.1 M phosphate buffer (PB) buffer (pH 7.4), post-fixed in 1% osmium tetroxide, dehydrated, critical-point dried and then sputter-coated. The samples were observed using a Hitachi S-4000 SEM (Hitachi, Ibaraki, Japan) with an acceleration voltage of 10 kV. For analyzing the samples using TEM, a drop of the suspension were deposited on

the TEM grid covered with a Formvar membrane, dried, and evacuated before the analysis. For root and leaf samples, the samples were fixed in 2.5% GA and 2% PA in 0.1 M PB buffer, pH 7.4, post-fixed in 1% osmium tetroxide, dehydrated, infiltrated with ethanol:Epon, embedded in pure Epon and polymerized at 60°C for 2 days. Ultra-thin sections were stained with 2% uranyl acetate and lead citrate. The preparations were observed using a Hitachi H-800 TEM. The acceleration voltage was 75 kV.

Chemicals used in this study were purchased from Kanto Chemical Co., Inc, Wako Pure Chemical Industries, Ltd., and Sigma Aldrich, Inc., Japan. Red spinach (*Amaranthus tricolor* L. and *Amaranthus lividus* L.) seeds were purchased from Dhaka, Bangladesh.

2.2. Hydroponic culture and effects of CNTs on the growth of red spinach

Seeds were sterilized (10 min) in a 10% sodium hypochlorite solution, washed with deionized water, and soaked overnight in CNTs solution (0, 125, 250, 500, and 1000 mg L^{-1}) in the dark at 25 °C. Seeds were then placed on filter paper with 3 mL test solution in covered Petri dishes and incubated at 25 °C in the dark until germination. After germination, seedlings were transferred to plastic pots (12 plants per pot) for 15 days

hydroponic culture; pots contained 200 mL Modified Hoagland medium [33] with and without CNTs (0, 125, 250, 500, and 1000 mg L^{-1}), with three replicates per treatment. In parallel, red spinach seedlings were also transferred to Hoagland medium supplemented with CNTs and AsA. At 1000 mg L^{-1}, the CNTs solution was stable with very little settling. Solutions were manually agitated before use. The pH of media was adjusted to 6.0 and remained unchanged with time. After 15 days of treatment, the plants' roots and shoots were separated, washed with water to remove the growth medium, and dried with a kimwipe to remove the surface water. Their lengths and fresh weights were recorded. Leaf numbers were counted and leaf areas (two plants leaf per pot) measured using a RHIZO 1004b instrument. We performed same experiment with carbon black as positive control.

2.3. Effect of CNTs on cell death (Evans blue and electrolyte leakage)

The cell death of CNTs-treated and untreated plant roots was tested as previously described by Baker and Mock [34], using Evans blue after 15 days of exposure. Cell death was measured spectroscopically after extraction of the Evans blue using 1% (w/v) SDS (sodium dodecyl sulfate) in 50% (v/v) methanol at 50 °C for 15 min. The absorbance of the extracted solution was obtained at a wavelength of 597 nm (V-530

UV/UISNIR Spectrophotometer, Jasco, Japan). Cell death was expressed as absorbance of treated roots in relation to untreated roots (control).

Cell death was also evaluated by measurement of ion leakage from leaves. The percent of membrane injury was measured from the electrolyte leakage of treated and untreated plants by a conductivity method based on the procedure of Lutts et al. [35] and Begum et al. [28].

2.4. Detection of ROS (superoxide, hydrogen peroxide, and hydroperoxides)

We used nitro blue tetrazolium (NBT) salt, a chromogenic redox indicator, to demonstrate the generation and release of superoxide anion [36]. We used 3,3′-diaminobenzidine (DAB), to reveal hydrogen peroxide production [37] and we used the fluorogenic probe, 2′,7′-dichlorodihydrofluorescin diacetate (DCFH-DA), to detect hydroperoxides inside the cells [38]. CNTs-treated and untreated fresh leaves from 15-day-old plants were placed in NBT and DAB-HCl, incubated under vacuum for 2 h and ~8 h, respectively. An insoluble blue formazon compound was produced when NBT reacted with super oxide, and a deep reddish-brown polymerization product was produced when DAB reacted with H_2O_2; both could be visualized under a Transmit Light Microscope BX51 with an Olympus DP72 Camera after chlorophyll was removed

from the leaves by boiling 15 min in ethanol. The amount of deep reddish-brown polymerization product in leaves was measured spectrophotometrically at A_{700} (V-530 UV/UISNIR Spectrophotometer, Jasco, Japan) after leaves were ground in liquid nitrogen and solubilized in a mixture of 2 M KOH and DMSO at a ratio of 1:1.167 (v/v).

DCFH-DA was used for visualization and measurement of intracellular ROS by spectroscopy. Fresh leaves were incubated in DCFH-DA for 2 h for detection of ROS. After three PBS (phosphate-buffered saline) rinses, images were captured using fluorescence microscopy (Olympus IX70). We measured DCFH fluorescence intensity in the leaves using a spectrofluorometer (Hitachi F-4500) by suspending them in PBS buffer with an excitation wavelength at 485 nm and emission wavelength at 522 nm. The values were expressed as % of fluorescence intensity relative to control. This experiment was performed without exposure to light.

2.5. Localization of CNTs inside leaves using Raman spectroscopy

Fresh leaves were washed with distilled water several times and then dried at 60°C in an oven for one week and then analyzed using a Raman spectrometer. Vain and midrib areas were used. Raman scattering spectra were obtained with a Raman spectrometer

(inVia Raman Microscope RENISHAW, England) equipped with a charge-coupled detector and a 1800 l/mm grating. The excitation source was a diode laser (785 nm), focused with a 100× objective to an area of approximately 2 μm. Spectra were acquired in a single scan with an acquisition time of 500s. The spectra were analysed using WiRE3.2 software from Renishaw.

2.6. Statistical analysis

Each treatment was conducted in triplicate. Phytotoxicity endpoints for all measurements were compared to those of the untreated controls. Statistical analysis was performed using Student's t-test with $P \leq 0.01$ considered significant. All data are presented as mean ± SD (standard deviation).

3. Results and discussion

3.1. CNTs analysis

Fig. 1 shows the (a) SEM, (b) TEM micrographs of the CNTs before and after dissolving into the modified Hoagland medium and (c) AFM image of the CNTs before dissolving into the modified Hoagland medium, depicts the morphology of the

water-wetted milled CNTs that were used in this study. Determination of relative metal (Fe, Co, Ni, Mn and Cr) concentrations of CNTs using inductively coupled plasma mass spectrometer (ICP-MS, Seiko-SPQ-6500, Tokyo, Japan). Data on quantitative analysis of the metal impurities (ppm in weight) for CNTs before and after dissolving into the modified Hoagland medium, we obtained below the detection limit of Fe, Co, Ni, Mn and Cr, only in modified Hoagland medium, Fe=174.53 and Mn=455.75, because the hydroponic solution containing the Fe and Mn.

Fig. 1. here

3.2. Effects of CNTs on the growth of red spinach

We conducted a series of tests of the potential effects of the multi-walled CNTs on the seedling growth of red spinach. We performed same experiment with carbon black as control. Little or no effect of carbon black on parameters tested (seed germination and growth) was noted in our experiment. The following discussion is focused on the results obtained with CNTs. Compared to the untreated seeds; fully germinated seedlings with developed cotyledons and root system were retarded with increasing CNTs concentration, as shown in Fig. 2. Hydroponic exposure for 15 days to CNTs at different concentrations (0, 125, 250, 500 and 1000 mg L^{-1}) resulted in toxicity

symptoms and retardation of plant growth, leaf number, and size with increasing CNTs concentration compared to control plants (Fig. 3a). Leaf color was greatly affected by CNTs treatment; as compared to the control, the red pigment was reduced at all given treatments and greatly reduced at high CNTs concentrations (500 or 1000 mg L^{-1}) (Fig. 3b). The color of the leaf blade also changed dramatically with increasing CNTs levels; the leaves became yellow (senescence) with wilting symptoms and sometimes exhibited blade curling (Fig. 3b). It has been shown previously that the expression of senescence-enhanced genes can be induced in plants by an increase in ROS, turning leaves yellow [39].

Fig. 2. here

Fig. 3. here

Heights and fresh weights of roots and shoots were all substantially reduced with increasing CNTs doses over control (Fig. 4), which is in good correlation with the findings of Stampoulis et al. [40] regarding the impact of five NMs, including CNTs, on the seed germination, root elongation, and biomass of Zucchini. We found that, compared to the control plants, CNTs concentrations of 125, 250, 500, and 1000 mg L^{-1}, respectively, resulted in reduction in root height of 21%, 50%, 54%, and 68% (Fig. 4a);

shoot height reduction of 18%, 37%, 68%, and 73% (Fig. 4a); root weight decrease of 63%, 94%, 95%, and 96% (Fig. 4b); shoot weight decrease of 65%, 87%, 96%, and 97% (Fig. 4b); the number of leaves was reduced by 19%, 48%, 52%, and 57% (Fig. 4c); and leaf area was reduced by 63%, 84%, 95%, and 96% (Fig. 4d). All control plants developed seven leaves each and remained red and healthy during the 15 days, whereas treated plants exhibited reduced leaf number and area and altered leaf shape, as the area was more suppressed than the length. Based on these results, we concluded that the addition of CNTs into the Hoagland medium caused toxic symptoms/visible changes in the red spinach, with the intensity of symptoms correlating to increasing CNTs concentration. This was consistent with our previously reported finding [28] that the vegetative biomass production of red spinach was reduced and showed toxic symptoms with increasing carbon nanoparticles (graphene) compared to control plants.

Growth cessation of CNTs-treated plants may have been due to the major changes of root morphological parameters and destruction of root structure in response to various CNTs concentrations. Most of the previous studies reporting deleterious effects of CNTs on root growth were based merely on parameters like root elongation, fresh weights, and root hair [40] and [41]. The literature does report positive/negative effect

on seedling growth of higher plant species after exposure to carbon nanoparticles [28]. Nanoparticles toxicity depends on probably due to differences in root anatomy because xylem structures determine the speed of water transport and different xylem structures may demonstrate different uptake kinetics of nanoparticles [42].

Here we showed that plants can also respond to CNTs toxicity via changes in surface area, production or inhibition of lateral roots and tips, and variation in other morphological parameters.

Fig. 4. here

3.3. Cell death determination using Evans blue and electrolyte leakage

We used the Evans blue staining method to detect cell death in 15-day-old fresh roots grown hydroponically with 0–1000 mg L^{-1} CNTs. Fig. 5a shows the results obtained after staining the root with Evans blue and discoloring with methanol. Plants treated with CNTs showed a higher capacity to fix the dye in comparison with control plants, and the measurement of the Evans blue showed concentration dependent induction (Fig. 5a). Higher CNTs concentrations (500 and 1000 mg L^{-1}) caused 4.0- and 5.9-fold higher Evans blue uptake, respectively, compared to that in control roots. Whereas,

lower concentrations (125 and 250 mg L^{-1}) CNTs caused only 1.4- and 1.8-fold higher Evans blue uptake, respectively.

Fig. 5. here

We also used electrolyte leakage, an indicator of membrane damage, to show the extent of cell death. Fig. 5b shows that electrolyte started to leak from leaves treated with the lowest concentration of CNTs (125 mg L^{-1}). Thereafter, the % of electrolyte leakage progressively increased, reaching its highest level at 1000 mg L^{-1} of CNTs. These results demonstrated that CNTs induced toxicity-associated bio-effects that produced the dose-dependent effect in Evans blue uptake and electrolyte leakage, both indicating cell death. ROS accumulation reportedly causes cell death that can be demonstrated by electrolyte leakage from cells and rapid rise of Evans blue uptake [43] and [28]. Hence, the present findings suggest that intracellular ROS might have a crucial role in CNTs-mediated induction of cell death.

3.4. Oxidative stress assay

ROS are key signalling molecules that can be induced by many exogenous stimuli [29]. We used ROS-sensitive dyes (DAB, NBT, and DCFH-DA) to evaluate the ROS accumulation induced by CNTs in 15-day-old fresh red spinach leaves. Compared to

controls, infiltration of CNTs-treated leaves with DAB and NBT resulted in deep reddish-brown polymerization (Fig. 6a–b) and blue formazon (Fig. 6d–e) respectively. This indicated the accumulation of H_2O_2 and super oxide, respectively, identifying cells in which the respective production rates were significantly greater than the detoxification rates.

Fig. 6. here

Infiltration of leaves with DCFH-DA allowed the detection of hydroperoxides. In untreated leaves there were few cells with fluorescence spots; fluorescence spots were significantly increased with increasing CNTs level (1000 mg L^{-1}) (Fig. 6g–h), meaning that more cells were stressed and dead. This confirmed the results of DAB and NBT staining, that epidermis cells were experiencing oxidative stress. Measurement of DAB polymerization and DCFH fluorescence by spectrofluorometer demonstrated the increase in ROS content in CNTs-treated leaves (Fig. 6j–k) compared to control respectively. These results show an involvement of ROS in CNTs-induced cell death and correspond to previous findings regarding CNTs-potentiated ROS production in rice cell suspension [20]. Our results indicate that CNTs elicit ROS production that

appears to be required for phytotoxicity and precedes cell death via an apoptotic pathway or by necrosis.

3.5. AsA treatment

The above DAB, NBT, and DCFH-DA-based imaging (Fig. 6) indicated that CNTs induced a burst of ROS in susceptible plant leaves. ROS overproduction induced by carbon nanoparticles is a key elicitor of cell death [28]. This suggests the potential for toxicity reversal through treatment with antioxidants that can neutralize the harmful effects of ROS [44]. We assessed ROS generation in plants with the presence of CNTs and the antioxidant AsA to characterize AsA's effect on CNTs-induced cell death and morphology changes. AsA is the most effective reducing substrate for ROS removal in plant cells [45]. Plants grown with CNTs (1000 mg L^{-1}) and supplemented with 1000 mg L^{-1} of AsA for 15 days were evaluated by DAB, NBT, and DCFH-DA staining, which confirmed almost complete protection (Fig. 6c, f, and i) against CNTs (1000 mg L^{-1})-induced ROS (Fig. 6b, e, and h). Spectroscopic measurement of DAB polymerization and DCFH fluorescence confirmed the decrease in ROS content in CNTs-treated leaves supplemented with 1000 mg L^{-1} of AsA (Fig. 6j–k) compared to control respectively. AsA is a membrane-permeable ROS scavenger [46] that

suppresses ROS accumulation in plants; AsA treatment protects roots from salt stress-induced tomato root death and associated oxidative damage and also inhibits ROS-dependent root gravitropism [47] and [48]. In our study, AsA treatment significantly suppressed the production of DAB polymerization (Fig. 6c and j), NBT formazon (Fig. 6f), and DCF fluorescence spots (Fig. 6i and k), compared to plant leaves treated with CNTs (1000 mg L^{-1}) alone (Fig. 6b, e, h, j and k). This indicates that oxidative stress is a major contributor to CNTs toxicity. AsA in combination with CNTs blocked the ROS increase, suggesting ROS inhibition as the mechanism of the observed resistance to CNTs-induced cell death, i.e., the antioxidant-defence mechanism. However, the exact mechanism involved in this resistance remains unclear.

The CNTs-treated plants exhibited toxic symptoms with severely decreased plant growth after 15 days, whereas plants treated with CNTs and AsA exhibited normal growth, similar to the Hoagland medium only control group (data not shown). AsA is not only important in protection of plant from being damaged by ROS; it also influences plant growth and development [49]. As one of the well-known powerful electron donors, AsA is capable of neutralizing superoxide, peroxide and hydroxyl, the key ROS [50-52].

The observation that AsA can inhibit CNTs-induced cell death is a major breakthrough. ROS-induced cell death is implicated in a number of developmental processes and stress responses, including leaf senescence, cell death of root cap cells, and some types of necrosis and HR, depending on the nature of the ROS species [53] and [54]. HR, a form of programmed cell death (PCD) occurs as a plant immune response to survive pathogen attack [55]. Dat et al. [54] and Jabs et al. [56] identified H_2O_2 and superoxide anion as initiators of PCD events and necrotic lesion formation, respectively. There is increasing evidence that various concentrations and durations of ROS exposure will lead to either necrosis or PCD [57] and [58]. Consequently, the cellular damage resulting from high ROS levels shows some typical hallmarks of necrosis, because phytotoxic levels of oxidants indiscriminately attack cellular constituents, leading to membrane leakage and cell lysis.

3.6. Morphological observation of leaves and roots using light microscopy and SEM.

Light microscopy and SEM were used to investigate leaf and root morphology. The 15-day-old plants grown in CNTs-enriched hydroponic culture showed significant differences in the thickness and color of the midrib tissues (Fig. 7a–e). In controls,

leaves were healthy with red coloration (Fig. 7a). Increasing CNTs levels correlated with the leaf blade and vein color changing from red to blackish (Fig. 7b–e). At the highest CNTs level, the red color disappeared.

Fig. 7. here

Control plants had roots with prolific root hairs, undamaged root caps, and intact epidermis (Fig. 7f). The first evidence of CNTs toxicity at low concentrations included reduced number and length of root hairs and deformation of root caps, higher concentrations led to impaired thickening, CNTs adsorbed to plant roots, and formation of lateral root (Fig. 7g–j). It was recently demonstrated that seedlings in the presence of nanoparticles failed to develop root hairs, had broken epidermis and root caps, and exhibited adsorption of nanoparticles on the root surface [28] and [59].

SEM analysis showed morphological evidence of broken midrib, with elongated, irregularly shaped cells and epidermis swelling at 500 mg L^{-1} CNTs (Fig. 8c–d). The epidermis and midrib of control leaves were smooth, regular in shape (Fig. 8a–b). Some stomata of the CNTs-treated red spinach leaves were identified as closed by SEM analysis (Fig. 8c). Stomata closure prevents water loss [60], leading to decreased CO_2 concentration inside the leaf. Lee et al. [61] demonstrated that pathogen-infected guard

cells may close their stomata via a pathway involving H_2O_2 production, thus interfering with the constant attack of pathogens through the stomatal pores. Plants commonly activate a variety of defence mechanisms against pathogen infection, often leading to production of ROS, such as superoxide and H_2O_2, which can in turn facilitate a hypersensitive response (HR) [62]. McAinsh et al. [63] observed that exogenously added superoxide and H_2O_2 inhibit stomatal opening and promote stomatal closing.

Fig. 8. here

The root surfaces of the control plants, observed by SEM, were properly developed (Fig. 8e–g). With CNTs (500 mg L^{-1}), the outer cell layers forming the epidermis underwent the greatest changes (Fig. 8h–l). Many root cells exhibited damaged cell walls and root cap, cracks, loss of tissue, and the detachment of the outer cell layers (Fig. 8h–i). We observed CNTs accumulation on the cell wall (Fig. 8i), which may cause damage. The root diameters were increased in the presence of CNTs, possibly as a result of water absorbtion by CNTs [14]. The lateral roots were developed to the mitosis zone (Fig. 8h, double arrow indicates mitosis zone). The substantially reduced length of red spinach root hairs in the presence of CNTs, particularly in the elongation regions, could cause the formation of lateral roots close to the mitosis zone

(apical part) of the primary root; this is corroborated by the findings of Clune & Copeland, [64] relating to other plant species. Moreover, we observed the beginnings of lateral roots within a very close distance of the root mitosis zone, as well as increased lateral root production in this layer and lateral root damage. The existing literature describes no cases where lateral roots grow in the mitosis zone under the influence of CNTs. This could have resulted from the quick drying-off of the outer cell layers, including the epiblema (the epidermal cells of rootlets, specially adapted to absorb liquids).

3.7. Morphological observations and localization of CNTs inside the roots and leaves using TEM and Raman spectroscopy

Typical features of dead cells were found in the CNTs-treated leaves, including cell membrane breakage (Fig. 9c, arrow), and collapse of the vacuole (Fig. 9d, arrow). Chloroplasts of control leaves exhibited well-developed granum, thylakoid structures, and membranes (Fig. 9a). Leaves treated with 500 mg L^{-1} CNTs exhibited granum and thylakoid degradation (Fig. 9b), membranes damaged (Fig. 9b, outer and inner membrane of chloroplast, arrow) implying that these chloroplasts were in a state of disruption. ROS generation assessed by DCFH-DA, DAB, and NBT confirmed the

direct presence of ROS generated inside the leaf in plants grown with CNTs. ROS generation, chloroplast disruption and rapid cell death are all characteristics of HR [65].

Fig. 9. here

Carbon nanomaterials can penetrate the cell wall and cell membrane of intact plant cells [14] and [15]. Based on the assumption that nanotubes can penetrate the root and then translocate into the leaf, TEM and Raman spectroscopy was used to detect CNTs inside the roots and leaves of the treated plants respectively. TEM and light microscopic image showing CNTs uptake inside the root (Fig. 9e, arrow) and leaf midrib area (Fig. 9f, square) cell of red spinach respectively.

The unique Raman spectrum of the CNTs and their strong scattering properties provide an exceedingly powerful tool for detecting graphitic materials, such as CNTs, inside a biological system [14]. The characteristic bands for CNTs are observed in the Raman spectra at 1330 cm^{-1}, 1590 cm^{-1}, and 2640 cm^{-1} due to the D-band, G′-band, and 2D-band, respectively (Fig. 9g). Our results clearly showed that CNTs could penetrate and translocate to different cellular compartments. Phytoremediation is a promising emerging technology. Red spinach that accumulates NMs in its roots and leaves,

represents promising potential for environment recovery to absorb NM pollutants from the environment.

4. Conclusions

In conclusion, our results provide clear experimental evidence that CNTs-induced growth reduction and toxicity are due to ROS. We found that CNTs cause HR-type necrotic lesions of leaf cells/tissue and changes of root and leaf morphology. ROS production is usually followed by the HR to pathogens, leading to rapid cell death (necrosis) [66]. It is well known that ROS generation can lead to protein, lipid, and DNA oxidation and to cell death [29], thereby preventing plant growth. The protection against CNTs-induced toxicity by the addition of AsA also supports that CNTs principally promote ROS generation. Using AsA in growth medium with CNTs reduced CNTs-induced browning/necrotic lesions of leaf tissue/cells and increased the growth to near that of the control plants, indicating potential applications for controlling ROS. Guidelines for the safe use of CNTs are critical issues in future studies, this shall include studies on the tolerance concentration for plants toward CNTs. Studies focussing on the use of plants for bioremediation of the nano-particle pollution is another topic being under taken in our groups.

Acknowledgments

We gratefully acknowledge Prof. Toru Miura and Prof. Shunitz Tanaka for providing necessary facilities during the study. We also gratefully acknowledge Yoshinobu Nodasaka and Natsumi Ushijima for their kind assistance in preparing the SEM and TEM samples. Many thanks go to Hongwen Yu for his assistance during the AFM and Raman spectroscopy study. The very helpful comments from the reviewers on the preliminary version of this paper are also gratefully acknowledged.

References

[1] S.R. Morrissey, Nanotechnology in food and agriculture, Chem. Eng. News 84 (2006) 31.

[2] A.M. Thayer, Carbon nanotubes by the metric ton: Anticipating new commercial applications, producers increase capacity, Chem. Eng. News 85 (2007) 29–38.

[3] W. Luther (Editor), Industrial application of nanomaterials—chances and risks, Technology analysis VDI Technologiezentrum GmbH, Düsseldorf Futur Technologies 54, 2004, pp. 119.

[4] UBA (Umwelt Bundes Amt), Nanotechnology: Opportunities and risks for humans and the environment, 2006.

[5] K. Donaldson, C.L. Tran, An introduction to the short-term toxicology of respirable industrial fibres, Mutat. Res. 553 (2004) 5–9.

[6] R.F. Service, Nanotoxicology: Nanotechnology grows up, Science 304 (2004) 1732–1734.

[7] K.F. Soto, A. Carrasco, T.G. Powell, K. Garza, L. Murr, Comparative *in vitro* cytotoxicity assessment of some manufactured nanoparticulate materials characterized by transmission electron microscopy, J. Nanoparticle Res. 7 (2005) 145–169.

[8] J. Muller, F. Huaux, N. Moreau, P. Misson, J.F. Heilier, M. Delos, M. Arras, A. Fonseca, J.B. Nagy, D. Lison, Respiratory toxicity of multi-wall carbon nanotubes, Toxicol. Appl. Pharmacol. 201 (2005) 221-231.

[9] L. Braydich-Stolle, S. Hussain, J.J. Schlager, M.C. Hofmann, *In vitro* cytotoxicity of nanoparticles in mammalian germline stem cells, Toxicol. Sci. 88 (2005) 412-419.

[10] M. Lippmann Effects of fiber characteristics on lung deposition, retention, and disease, Environ Health Perspect. 88 (1990) 311–317.

[11] E. Roduner, Size matters: why nanomaterials are different**,** Chem. Soc. Rev. 35 (2006) 583

[12] K. Donaldson, V. Stone, Current hypotheses on the mechanisms of toxicity of ultrafine particles, Ann Ist Super Sanita. 39 (2003) 405-410.

[13] A.D. Maynard, P.A. Baron, M. Foley, A.A. Shvedova, E.R. Kisin, V. Castranova, Exposure to carbon nanotube material: aerosol release during the handling of unrefined single-walled carbon nanotube material, J. Toxicol. Environ. Health, 67 (2004) 87–107.

[14] M. Khodakovskaya, E. Dervishi, M. Mahmood, Y. Xu, Z. Li, F. Watanabe, A.S. Biris, Carbon nanotubes are able to penetrate plant seed coat and dramatically affect seed germination and plant growth, ACS Nano 3 (2009) 3221–3227.

[15] Q. Liu, B. Chen, Q. Wang, X. Shi, Z. Xiao, J. Lin, X. Fang, Carbon nanotubes as molecular transporters for walled plant cells, Nano Lett. 9 (2009) 1007–1010.

[16]M. Wierzbicka, D.M. Antosiewicz, How lead easily enters food chain—a study of plant roots, Sci. Total Environ. 1 (1993) 423–429.

[17] F. Torney, B.G. Trewyn, V.S-Y. Lin, K. Wang, Mesoporous silica nanoparticles deliver DNA and chemicals into plants, Nature Nanotech. 2 (2007) 295–300.

[18] L. Yang, D.J. Watts, Particles surface characteristics may play an important role in phytotoxicity of alumina nanoparticles, Toxicol. Lett. 158 (2005) 122–132.

[19] D.H. Lin, B.S. Xing, Phytotoxicity of nanoparticles: inhibition of seed germination and root growth, Environ. Pollut. 50 (2007) 243–250.

[20] X-m. Tan, C. Lin, B. Fugetsu, Studies on toxicity of multi-walled carbon nanotubes on suspension rice cells, Carbon 47 (2009) 3479–3487.

[21] C. Lin, B. Fugetsu, Y. Su, F. Watari, Studies on toxicity of multi-walled carbon nanotubes on *Arabidopsis* T87 suspension cells, J. Hazardous Mater. 170 (2009) 578–583.

[22] X-m. Tan, B. Fugetsu, Multi-walled carbon nanotubes interact with cultured rice cells: evidence of a self-defense response, J. Biochem. Nanotech. 3 (2007) 285–288.

[23] J.E. Canas, M.Q. Long, S. Nations, R. Vadan, L. Dai, M. Luo, R. Ambikapathi, E.H. Lee, D. Olszyk, Effects of functionalized and nonfunctionalized single-walled carbon nanotubes on root elongation of select crop species, Environ. Toxicol. and Chem. 27 (2008) 1922–1931.

[24] A.E. Porter, M. Gass, K. Muller, J.N. Skepper, P.A. Midgley, M. Welland, Direct imaging of single-walled carbon nanotubes in cells, Nature Nanotech. 2 (2007) 713–717.

[25] C.A. Poland, R. Duffin, I. Kinloch, A. Maynard, W.A.H. Wallace, A. Seaton, V. Stone, S. Brown, W. MacNee, K. Donaldson, Carbon nanotubes introduced into the abdominal cavity of mice show asbestos-like pathogencity in a pilot study, Nature Nanotech. 3 (2008) 423–428.

[26] S. Kang, M. Herzberg, D.F. Rodrigues, M. Elimelech, Antibacterial effects of carbon nanotubes: size does matter, Langmuir 24 (2008) 6409–6413.

[27] A. Nel, T. Xia, L. Madler, N. Li, Toxic potential of materials at the nanolevel, Science 311 (2006) 622–627.

[28] P. Begum, R. Ikhtiari, B. Fugetsu, Graphene phytotoxicity in the seedling stage of cabbage, tomato, red spinach, and lettuce, Carbon 49 (2011) 3907–3919.

[29] K. Apel, H. Hirt, Reactive oxygen species: metabolism, oxidative stress, and signal transduction, Annu. Rev. Plant Biol. 55 (2004) 373–399.

[30] G. Xiao, M. Wang, N. Li, J.A. Loo, A.E. Nel, Use of proteomics to demonstrate a hierarchical oxidative stress response to diesel exhaust particle chemicals in a macrophage cell line, J. Biol. Chem. 278 (2003) 50781–50790.

[31] P. Begum, R. Ikhtiari, B. Fugetsu, M. Matsuoka, T. Akasaka, F. Watari, Phytotoxicity of multi-walled carbon nanotubes assessed by selected plant species in the seedling stage, Appl. Surf. Sci. (2012) Article in press, DOI information: 10.1016/j.apsusc.2012.03.028

[32] S. Zhang, J. Liu, X. Bao, K. Niu, Seed-to-seed potential allelopathic effects between *Ligularia virgaurea* and native grass species of Tibetan alpine grasslands, Ecol. Res. 26 (2011) 47–52.

[33] D.R. Hoagland, D.I. Arnon, The water culture method for growing plants without soil, The College of Agriculture, University of California, California Agriculture Experiment Station Circular 347, Berkeley, 1950, pp. 1–32.

[34] C.J. Baker, N.M. Mock, An improved method for monitoring cell death in cell suspension and leaf disc assays using Evans blue, Plant Cell Tissue Org. Cult. 39 (1994) 7–12.

[35] S. Lutts, J.M. Kinet, J. Bouharmont, NaCl-induced senescence in leaves of rice (*Oryza sativa* L.) cultivars differing in salinity resistance, Ann. Bot. 78 (1996) 389±398.

[36] N. Doke, Involvement of superoxide anion generation in hypersensitive response of potato tuber tissues to infection with an incompatible race of *Phytophtora infestans*, Physiol. Plant Pathol. 23 (1983) 345–357.

[37] R.C. Graham, M.J. Karnowsky, The early stages of absorption of injected horseradish peroxidase in the proximal tubules of mouse kidney: ultrastructural cytochemistry by a new technique, J. Histochem. Cytochem. 14 (1966) 291–302.

[38] B. Naton, K. Hahlbrock, E. Schmelzer, Correlation of rapid cell death with metabolic changes in fungus-infected, cultured parsley cells, Plant Physiol. 112 (1996) 433–444.

[39] L.A. del Río, G.M. Pastori, J.M. Palma, F. Sevilla, F.J. Corpus, A. Jimenéz, E. López-Huertas, J.A. Hernandéz, The activated oxygen role of peroxisomes in senescence, Plant Physiol. 116 (1998) 1195–1200.

[40] D. Stampoulis, S.K. Sinha, J.C. White, Assay-dependent phytotoxicity of nanoparticles to plants, Environ. Sci. Technol. 43 (2009) 9473–9479.

[41] G. Ghodake, Y.D. Seo, D. Park, S. Lee, Phytotoxicity of carbon nanotubes assessed by *Brassica Juncea* and *Phaseolus Mungo*, J. Nanoelectron. and Optoelectron. 5 (2010) 157–160.

[42] C.W. Lee, S. Mahendra, K. Zodrow, D. Li, Y.C. Tsai, J. Braam, P.J.J. Alvarez, Developmental phytotoxicity of metal oxide nanoparticles to *Arabidopsis thaliana*, Environ. Toxicol. Chem. 29 (2010) 669–675.

[43] M. Kawai-Yamada, Y. Ohori, H. Uchimiya, Dissection of Arabidopsis Bax inhibitor-1 suppressing Bax-, hydrogen peroxide-, and salicylic acid-induced cell death, Plant Cell 16 (2004) 21–32.

[44] R. Cohen-Kerem, G. Koren, Antioxidants and fetal protection against ethanol teratogenicity I. Review of the experimental data and implications to humans, Neurotoxicol. and Teratol. 25 (2003) 1–9.

[45] G. Noctor, C.H. Foyer, Ascorbate and glutathione: Keeping active oxygen under control, Annu. Rev. Plant Physiol. Plant Mol. Biol. 49 (1998) 249–279.

[46] C.H. Foyer, Redox homeostasis and antioxidant signaling: a metabolic interface between stress perception and physiological responses, The Plant Cell 17 (2005) 1866–1875.

[47] J.H. Joo, Y.S. Bae, J.S. Lee, Role of auxin-induced reactive oxygen species in root gravitropism, Plant Physiol. 126 (2001) 1055–1060.

[48] A. Shalata, P.M. Neumann, Exogenous ascorbic acid (vitamin C) increases resistance to salt stress and reduces lipid peroxidation, J. Exp. Bot. 52 (2001) 2207–2211.

[49] C.H. Foyer, G. Kiddle, P. Verrier, Transcriptional profiling approaches to understanding how ascorbate regulates growth and the cell cycle, In: Baginsky S, Fernie AR, eds, Plant systems biology, Basel: Birkenhauser, 2006.

[50] M. Simkó, A. Gazsó, U. Fiedeler, M. Nentwich, Nanoparticles, free radicals and oxidative stress, NanoTrust Dossier, (2011) 012en

[51] H. Sies, Oxidative stress: Oxidants and antioxidants, Exp. Physiol., 82 (1997) 291-295.

[52] D. Nijs, P.M. Kelley, Vitamins C and E denote single hydrogen atoms in vivo, FEBS Lett. 284 (1991) 147–151.

[53] I. Gadjev, J.M. Stone, T.S. Gechev, Programmed cell death in plants: new insights into redox regulation and the role of hydrogen peroxide, Int. Rev. of Cell and Mol. Biol. 270 (2008) 87–144.

[54] J.F. Dat, N. Capelli, F.V. Breusegem, The interplay between salicylic acid and reactive oxygen species during cell death in plants, Biomedical and Life Sciences, Salicylic Acid-A Plant Hormone, 2007, pp. 247-276, DOI: 10.1007/1-4020-5184-0_9.

[55] Y. Liu, M. Schiff, K. Czymmek, Z. Tallóczy, B. Levine, S.P. Dinesh-Kumar, Autophagy regulates programmed cell death during the plant innate immune response, Cell 121 (2005) 567–577.

[56] T. Jabs, R.A. Dietrich, J.L. Dangl, Initiation of runaway cell death in an Arabidopsis mutant by extracellular superoxide, Science 273 (1996) 1853–1856.

[57] P.F. McCabe, A. Levine, P.J. Meijer, N.A. Tapon, R.I. Pennell, A programmed cell death pathway activated in carrot cells cultured at low cell density, The Plant J. 12 (1997) 267–280.

[58] V. Houot, P. Etienne, A.S. Petitot, S. Barbier, J.P. Blein, L. Suty, Hydrogen peroxide induces programmed cell death features in cultured tobacco BY-2 cells, in a dose-dependent manner, J. Exp. Bot. 52 (2001) 1721–1730.

[59] L. Yin, Y. Cheng, B. Espinasse, P.B. Colman, M. Auffa, M. Wiesner, J. Rose, J. Liu, S.E. Bernhardt, More than the ions: The effects of silver nanoparticles on *Lolium multiflorum*, Environ. Sci. Technol. 45 (2011) 2360–2367.

[60] U. Zimmermann, H. Schneider, L. Wegner, H.J. Wagner, M. Szimtenings, A. Haase, F.W. Bentrup, What are the driving forces for water lifting in the xylem conduit? Plant Physiol. 114 (2002) 327–335.

[61] S. Lee, H. Choi, S. Suh, I.S. Doo, K.Y. Oh, E.J. Choi, A.T.S. Taylor, P.S. Low, Y. Lee, Oligogalacturonic acid and chitosan reduce stomatal aperture by inducing the evolution of reactive oxygen species from guard cells of tomato and Commelina communis, Plant Physiol. 121 (1999) 147–152.

[62] A. Levine, R. Tenhaken, R.A. Dixon, C. Lamb, H_2O_2 from the oxidative burst orchestrates the plant hypersensitive response, Cell 79 (1994) 583–593.

[63] M.R. McAinsh, H. Clayton, T.A. Mansfield, A.M. Hetherington, Changes in stomatal behavior and cytosolic free calcium in response to oxidative stress, Plant Physiol. 111 (1996) 1031–1042.

[64] T.S. Clune, L. Copeland, Effects of aluminum on canola roots, Plant Soil 216 (1999) 27–33.

[65] L.A.J. Mur, P. Kenton, A.J. Lioyd, H. Ougham, E. Prats, The hypersensitive response; the centenary is upon us but how much do we know? J. Exp. Bot. 59 (2008) 501–520.

[66] J.T. Greenberg, A. Guo, D.F. Klessig, F.M. Ausubel, Programmed cell death in plants: a pathogen-triggered response activated coordinately with multiple defense functions, Cell 77 (1994) 551–563.

Captions for Figures

Fig. 1. (a) SEM, (b) TEM micrographs of the multi-walled CNTs before and after dissolving into the modified Hoagland medium and (c) AFM image of the CNTs before dissolving into the modified Hoagland medium.

Fig. 2. Digital image of red spinach seeds after incubation with and without CNTs solution on filter paper for 5 days at 25 °C in the dark.

Fig. 3. Morphological observations of seedlings exposed to CNTs (0-1000 mg L^{-1}) for 15 days. Digital image of (a) mature plants (b) leaves at different concentrations of CNTs.

Fig. 4. Effects of CNTs (0-1000 mg L^{-1}) on seedling growth. (a) Root and shoot length, (b) root and shoot weight, (c) leaf number, and (d) leaf area. Error bars represent standard deviation. Results are shown as means ± SD of 3 individual experiments.

Fig. 5. Effects of CNTs on root (a, Evans blue) and leaf (b, electrolyte leakage) cell death after 15 days. Error bars represent standard deviation. Results are shown as means ± SD of 3 individual experiments.

Fig. 6. Detection of ROS in growing leaves. 15 day-old fresh leaves treated with CNTs (0 and 1000 mg L^{-1}) were used. (a–b) Staining using the 3–3'-diaminobenzidine (DAB) (40x). (d-e) Staining using the NBT (40x). (g-h) Staining with DCFH-DA (4x). (c, f and i) Plants were grown with CNTs (1000 mg L^{-1}) and supplemented with 1000 mg L^{-1} of AsA for 15 days were used to compare the effects of AsA. (c) Staining with DAB (40x), (f) staining with NBT (40x), and (i) staining with DCFH-DA (4x). (j and k) Effect of CNTs (1000 mg L^{-1}) on accumulation of H_2O_2 and hydroperoxides in treated leaves as measured using DAB and DCFH fluorescence respectively.

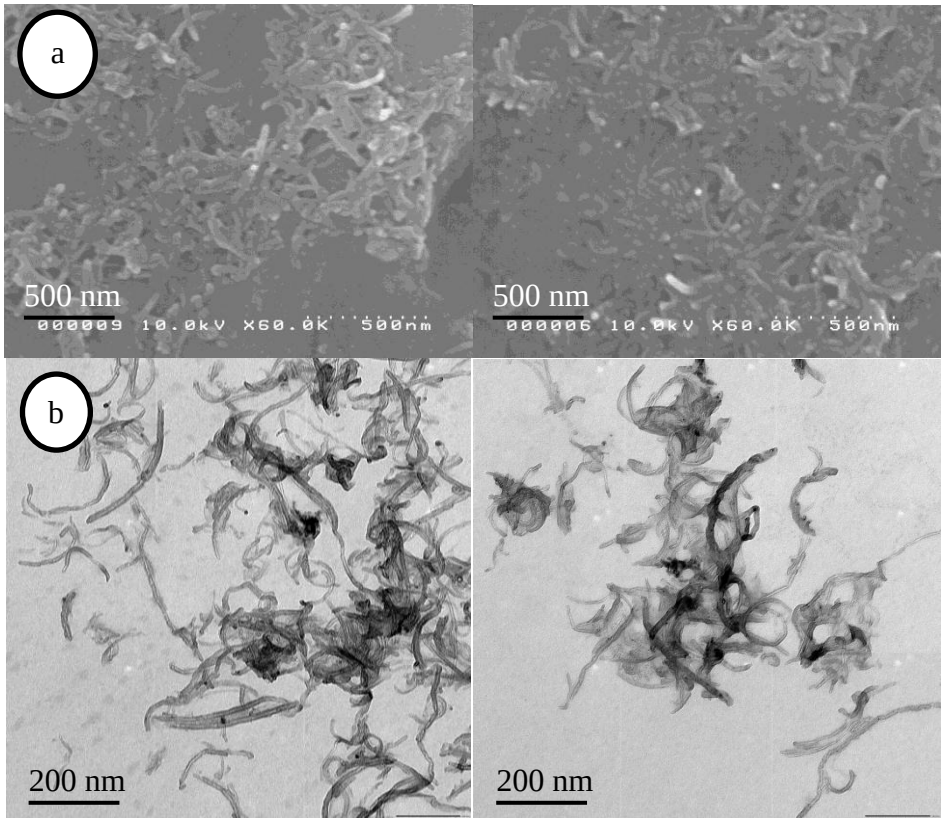
Fig. 7. Light microscopic picture of 15 day-old leaves (a-e, 10x) and roots (f-j, 10x).

Fig. 8. SEM observation of control and CNTs treated (500 mg L^{-1}) leaf. Control leaf (a) epidermis and (b) midrib, treated leaf (c) epidermis and (d) midrib. Control root (e) root cap and elongation zone, (f-g) root hair zone. Treated (h) root cap and elongation zone (white double arrow indicates mitosis zone), (i) root epidermis and (j) root hair zone. (k) Lateral root, (l) magnified root hairs zone.

Fig. 9. TEM of control and CNTs treated (500 mg L^{-1}) leaf and root. Control leaf (a) chloroplast, treated leaf (b) chloroplast, (c) cell membrane and (d) vacuole. Uptake of CNTs (e, arrow) by plant root cell. Light microscopic image of treated (500 mg L^{-1})

leaf (f, 40x). Raman spectrum of treated (500 mg L^{-1} CNTs) leaf obtained from 785 nm laser (g).

Fig. 1.



Before After

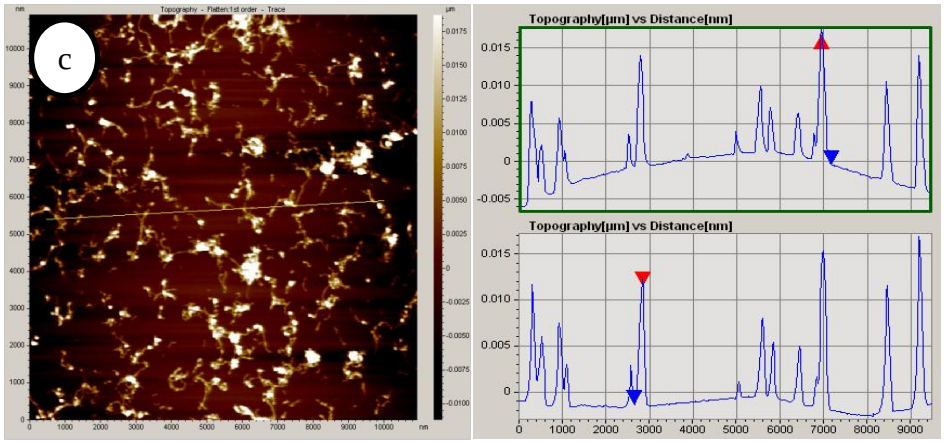


Fig. 2.



Control 125 250 500 1000

Concentrations of CNTs (mg/L)

Fig. 3.



Control 125 250 500 1000

Concentrations of CNTs (mg/L)

Fig. 4.

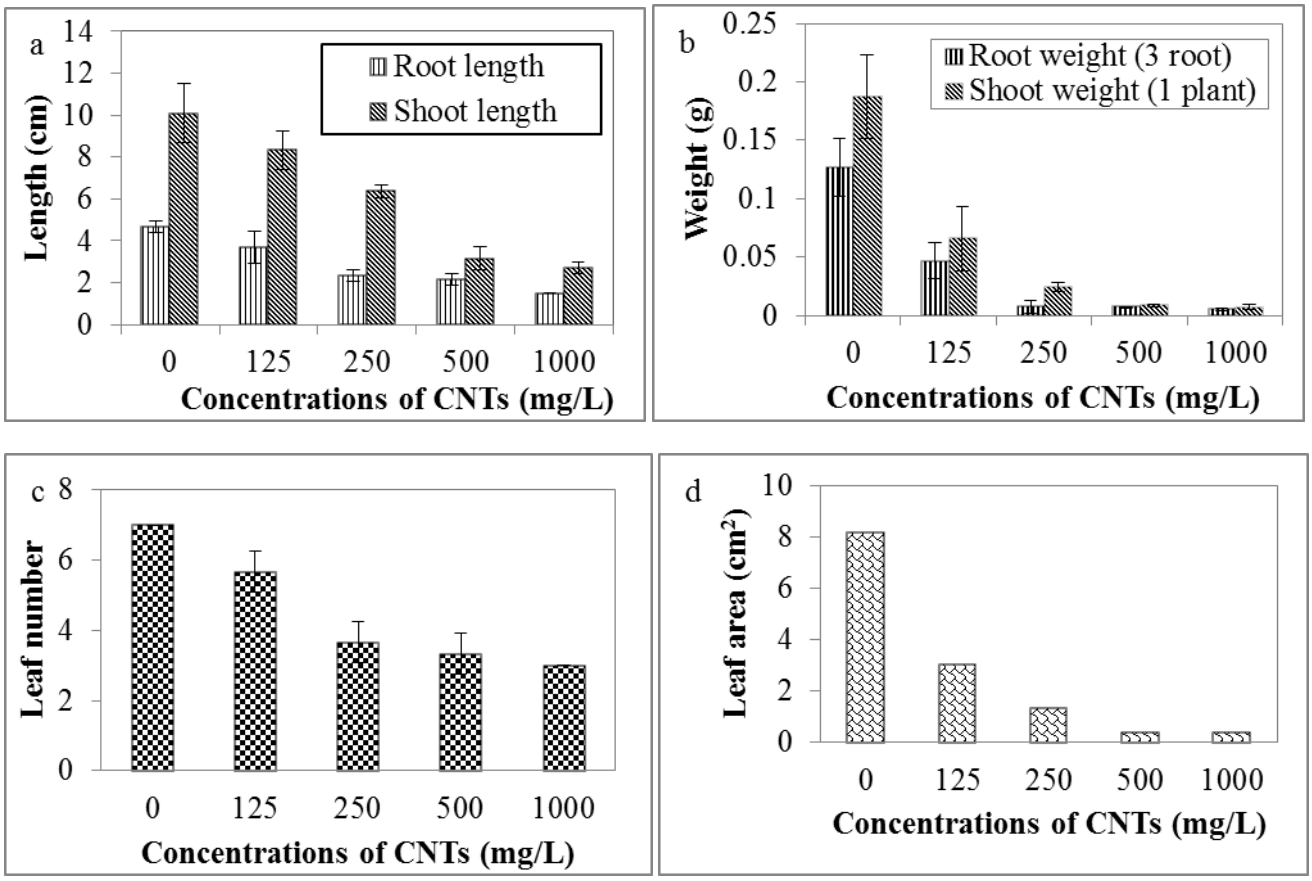

a
Length (cm)
Root length
Shoot length
Concentrations of CNTs (mg/L)
b
Weight (g)
Root weight (3 root)
Shoot weight (1 plant)
Concentrations of CNTs (mg/L)
c
Leaf number
Concentrations of CNTs (mg/L)
d
Leaf area (cm²)
Concentrations of CNTs (mg/L)

Fig. 5.

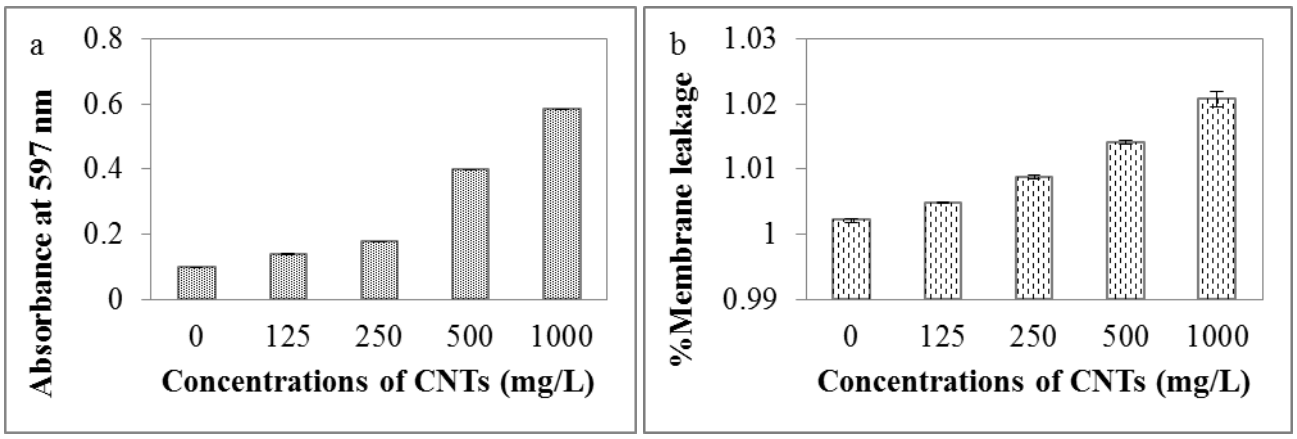

a
Absorbance at 597 nm
0.8
0.6
0.4
0.2
0
0
125
250
500
1000
Concentrations of CNTs (mg/L)
b
%Membrane leakage
1.03
1.02
1.01
1
0.99
0
125
250
500
1000
Concentrations of CNTs (mg/L)

Fig. 6.

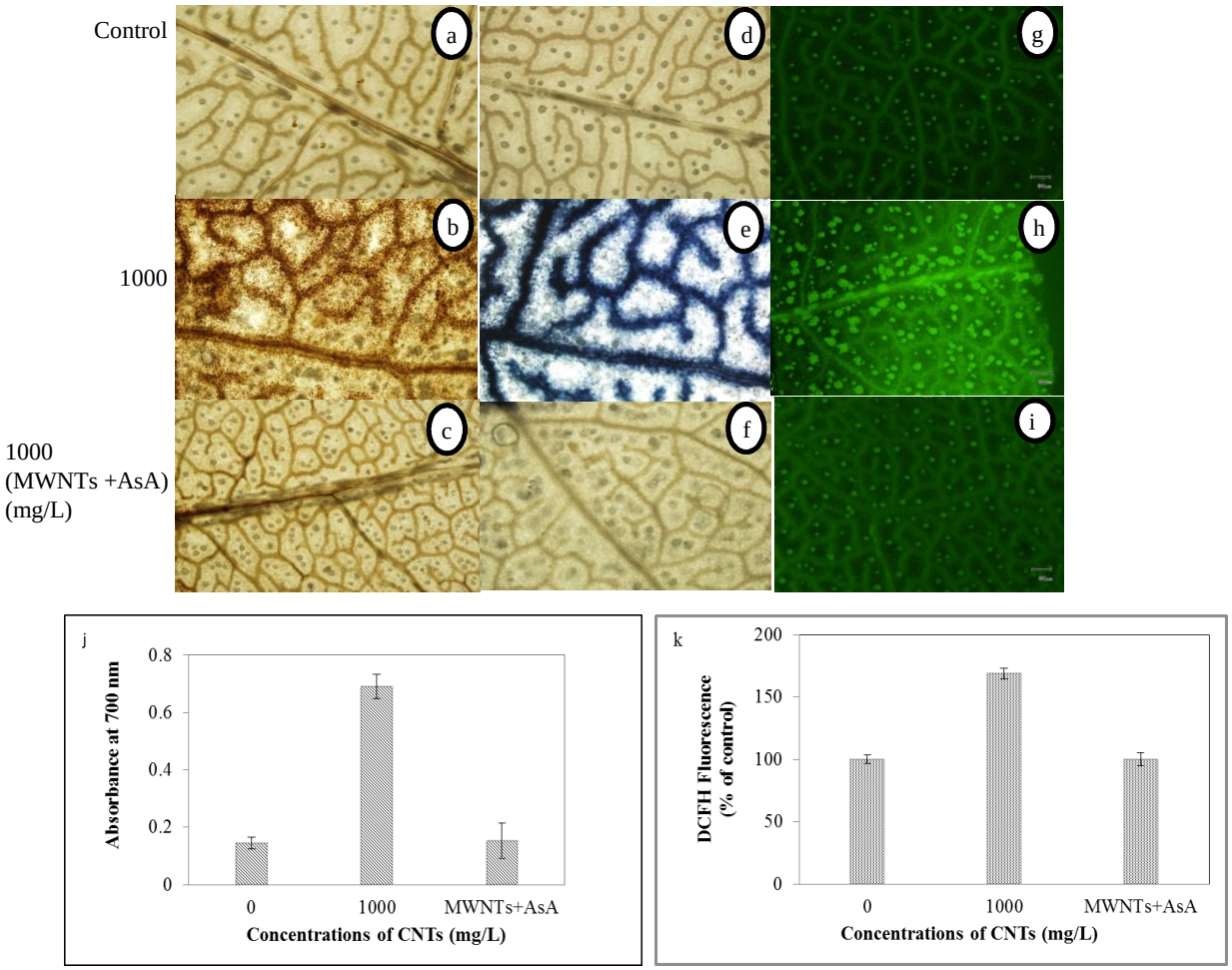

Control
1000
1000
(MWNTs +AsA)
(mg/L)
a
b
c
d
e
f
g
h
i
j
Absorbance at 700 nm
0
0.2
0.4
0.6
0.8
0
1000
MWNTs+AsA
Concentrations of CNTs (mg/L)
k
DCFH Fluorescence
(% of control)
0
50
100
150
200
0
1000
MWNTs+AsA
Concentrations of CNTs (mg/L)

Fig.7.

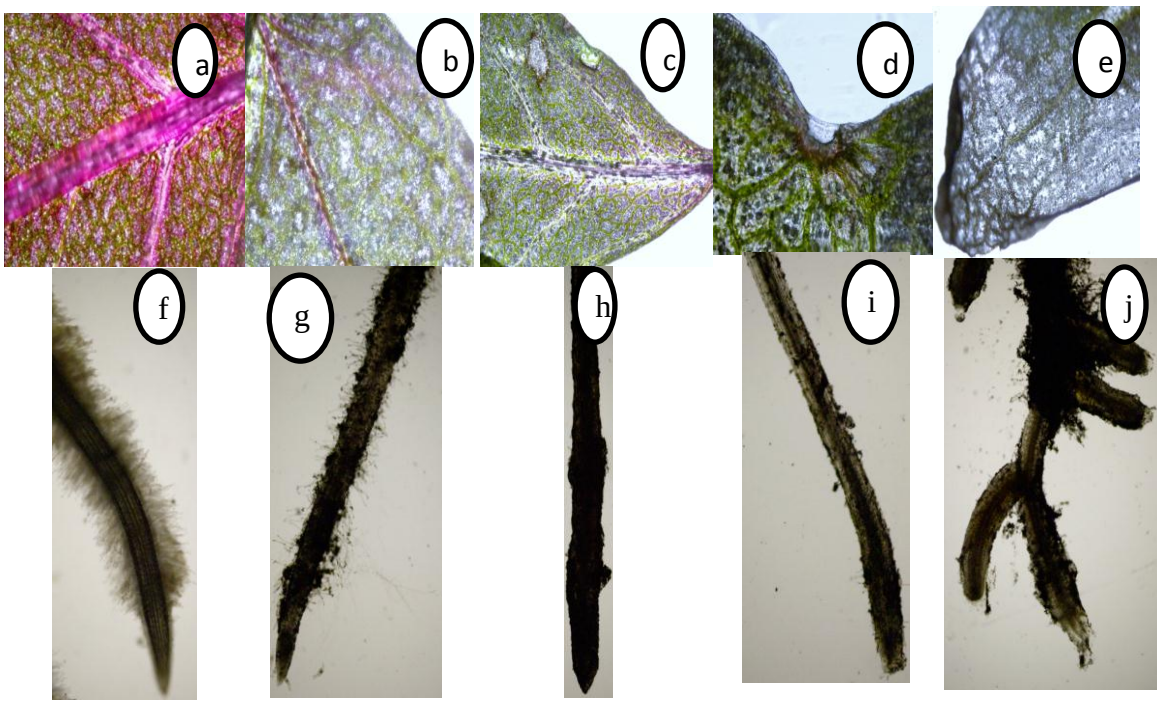

a
b
c
d
e
f
g
h
i
j
Control
125
250
500
1000
Concentrations of CNTs (mg/L)

Fig. 8.

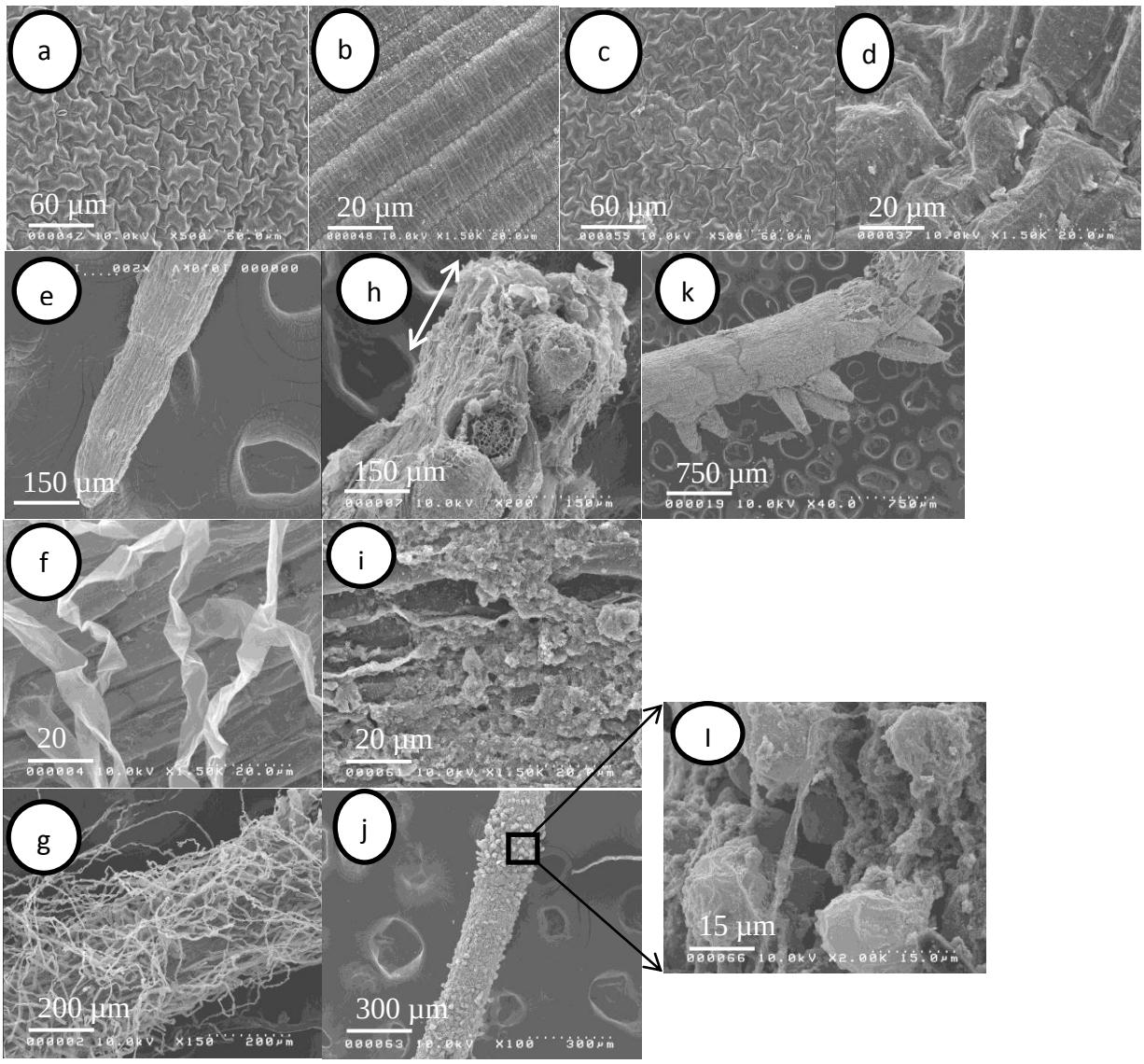

a
60 µm
b
20 µm
c
60 µm
d
20 µm
e
150 µm
h
150 µm
k
750 µm
f
20
i
20 µm
l
15 µm
g
200 µm
j
300 µm

Fig. 9.

